Wave-vector mismatch effects in electromagnetically induced transparency in Y-type systems

Azeem B. Mirza and Suneel Singh*
School of Physics, University of Hyderabad, Hyderabad 500 046, India
(Received 9 March 2012; published 29 May 2012)

We study electromagnetically induced transparency (EIT) of a probe field in a four-level Y-type atomic system driven by two strong laser (coupling) fields. Both homogeneously (radiative) and Doppler broadened systems are considered. The effect of residual Doppler broadening on EIT is demonstrated for various wave-vector mismatches occurring when the frequency of coupling fields is equal ($k_c = k_p$), higher ($k_c > k_p$), or lesser ($k_c < k_p$) than that of the probe field frequency. Contrary to usual belief it is found that for the $k_c > k_p$ wave-vector mismatch case, the probe absorption profile displays very wide and almost complete single or double EIT windows whose width, depth, and location depend upon the wave-vector mismatch, Rabi frequencies, and atom field detuning of the coupling fields. Analytical results are also obtained to explain these interesting features.

DOI: 10.1103/PhysRevA.85.053837 PACS number(s): 42.50.Gy, 42.50.Ct, 42.50.Hz

I. INTRODUCTION

Electromagnetically induced transparency (EIT) [1] is one of the many unusual and interesting phenomena produced by atomic coherence and interference effects that enable propagation (without significant attenuation) of light through an otherwise opaque atomic medium. EIT is of tremendous interest due to possibility of wide applications in optical switching via light velocity control [2], quantum information [3], and nonlinear optics [4].

Initial works on EIT primarily focused on one-photon transitions between states of opposite parity in simple three-level Λ, V, and cascade (ladder) systems [1–4]. However, currently there is considerable interest in the study of EIT and its effect on nonlinear optical interactions in four-level systems of various configurations. Pertinent to the present work is a four-level Y-type system interacting with two strong laser (coupling) fields and a low-intensity probe field.

Agarwal and Harshawardhan [5] predicted theoretically that a Y-type atomic system under one strong-field and two weak-field excitations can give rise to interesting effects such as inhibition and enhancement of the two-photon absorption. This effect was first experimentally observed by Gao *et al.* in sodium atoms [6] and subsequently electromagnetically induced *two-photon transparency* was experimentally observed in both ^{85}Rb and ^{87}Rb atomic vapors [7]. In a similar model, the resonance fluorescence [8] and vacuum-induced interference effects [9] were also investigated theoretically. Experimental observation of competing four-wave mixing (FWM) and six-wave mixing (SWM) processes [10] and two FWM processes [11] due to atomic coherence and interference in the four-level Y-type atomic systems were also reported. These experiments utilized two-photon Doppler-free configurations for propagation of the (pump, coupling, and probe) laser beams in an atomic Rb vapor cell. More recently a theoretical study of dynamical control of soliton formation and propagation [12] in a four-level Y-type homogeneously broadened system interacting with two strong laser fields and a low-intensity probe field was reported.

In atomic vapors the probe transparency (or absorption) characteristics are governed by the nature of the residual (two-photon) Doppler broadening originating from the thermal motion of the atoms and mismatch $k_p - k_c$, of applied probe and coupling field wave vectors k_p and k_c, respectively [13–15]. It is the usual belief that a Doppler-free medium is essential for observing reduced probe absorption at much lower coupling (or pump) laser power. Hence most experiments tend to utilize a two-photon Doppler-free geometry where the coupling and probe beams are counterpropagating and have similar frequencies so that $k_p = k_c$ and the residual Doppler width vanishes. Realizing perfect Doppler-free two-photon transition in real atomic systems is not feasible due to a rather large dissimilarity between the wavelengths (or wave vectors) of the (upper) transition driven by coupling field(s) and the lower transition connected by the probe field. Even the often-utilized nearly-Doppler-free two-photon process involving the $5\,s_{1/2} \rightarrow 5\,p_{3/2} \rightarrow 5\,d_{5/2}$ (or $5\,d_{3/2}$) transition in Rb [10,11] has a nonzero ($k_p < k_c$) residual width of 1.6 MHz [14], which is much larger than the dephasing rate (0.4 MHz) of the two-photon transition and thus can significantly affect the probe transparency. On the other hand it was found that the $k_p < k_c$ case is actually conducive to the observation of reduced probe absorption [13,15]. However, in the opposite $k_p > k_c$ (frequency upconversion) case, where no transparency can occur for a single coupling field, Silva *et al.* [16] demonstrated that using a standing-wave configuration of counterpropagating coupling fields, it is possible to induce a large transparency in a three-level cascade system whenever the ratio of probe to drive field frequency is close to half integer values. It therefore would be of interest to assess the influence of the various broadening mechanisms and different regimes of wave-vector mismatches in the inhomogeneous broadening case (particularly when $k_p < k_c$) on probe transparency (absorption) characteristics in a Y-type four-level system.

In this work we study the transparency of a weak probe field in a Doppler broadened four-level Y-type system interacting with two strong laser (coupling) fields. To compare and contrast, an analysis of a homogeneously (radiatively) broadened four-level Y-type system is also presented. The organization of the paper is as follows: Sec. II (which also contains several subsections) deals with density-matrix formulation. We solve for the steady-state density-matrix equations for

*suneelsp@uohyd.ernet.in

the Y-type system to first order in amplitude of a (weak) probe field. Expressions are derived for one-photon (probe) coherence, susceptibility, and absorption coefficients from which absorption and dispersion characteristics of the probe field can be determined. Analytical results are derived so as to explain the influence of various broadening mechanisms as well the velocity selective nature of the probe transparency in different regimes of wave-vector mismatch. It is shown that depending on the amplitude and the detuning of the coupling lasers, the absorption profile of a weak probe field shows single or double EIT windows whose location, width, and depth can be controlled by manipulating the parameters of the coupling fields. In Sec. III numerical results are presented for probe absorption and dispersion considering the transitions $3\,S_{1/2} \rightarrow 3\,P_{3/2} \rightarrow 4\,D_{3/2}$ ($3\,S_{1/2} \rightarrow 3\,P_{3/2} \rightarrow 4\,D_{5/2}$) in a sodium atom. These are compared with the analytical results derived in the previous section and good agreement is obtained. A brief summary and conclusions are presented in Sec. IV.

II. THEORY FOR THE Y SYSTEM

A. Formulation

We consider a dual ladder Y-type four-level atomic system interacting with three laser fields $\vec{E}_p$, $\vec{E}_{c1}$, and $\vec{E}_{c2}$ as shown in Fig. 1. The spontaneous emission rates from the two nearly degenerate upper states $|4\rangle$ and $|3\rangle$, respectively, to intermediate level $|2\rangle$ are $2\gamma_{42}$ and $2\gamma_{32}$, and that from level $|2\rangle$ to ground level $|1\rangle$ is $2\gamma_{21}$. The three laser fields are given by $\vec{E}_p = \vec{\varepsilon}_p \exp[i(\vec{k}_p \cdot \vec{r} - \omega_p t)] + \text{c.c.}$, $\vec{E}_{c1} = \vec{\varepsilon}_{c1} \exp[i(\vec{k}_{c1} \cdot \vec{r} - \omega_{c1} t)] + \text{c.c.}$, and $\vec{E}_{c2} = \vec{\varepsilon}_{c2} \exp[i(\vec{k}_{c2} \cdot \vec{r} - \omega_{c2} t)] + \text{c.c.}$. The weak probe laser field

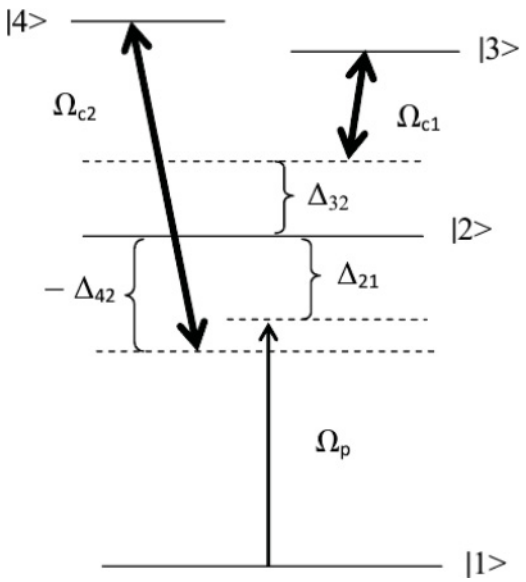

FIG. 1. EIT scheme in a four-level Y-type atomic system with dual ladder-type EIT. Here Ω_p is the Rabi frequency of the (weak) probe and Ω_{c1}, and Ω_{c2} are the (strong) coupling field Rabi frequencies. The detunings of the probe and coupling fields from their respective atomic transitions are $\Delta_{21} = \omega_{21} - \omega_p$, $\Delta_{32} = \omega_{32} - \omega_{c1}$, and $\Delta_{42} = \omega_{42} - \omega_{c2}$, respectively.

$\vec{E}_p$ of frequency ω_p, wave vector $\vec{k}_p$, and Rabi frequency $\Omega_p = (\vec{\mu}_{21} \cdot \vec{\varepsilon}_p)/\hbar$ is applied to the $|1\rangle \rightarrow |2\rangle$ transition. The transition $|2\rangle \rightarrow |3\rangle$ ($|2\rangle \rightarrow |4\rangle$) is being driven by the coupling laser field $\vec{E}_{c1}$ ($\vec{E}_{c2}$) of frequency ω_{c1} (ω_{c2}), the wave vector $\vec{k}_{c1}$ ($\vec{k}_{c2}$), and the Rabi frequency $\Omega_{c1} = (\vec{\mu}_{32} \cdot \vec{\varepsilon}_{c1})/\hbar$ [$\Omega_{c2} = (\vec{\mu}_{42} \cdot \vec{\varepsilon}_{c2})/\hbar$]. Here $\vec{\mu}_{21}$, $\vec{\mu}_{32}$, and $\vec{\mu}_{42}$ are dipole moments of the $|2\rangle \rightarrow |1\rangle$, $|3\rangle \rightarrow |2\rangle$, and $|4\rangle \rightarrow |2\rangle$ transitions, respectively.

The interaction Hamiltonian in the interaction picture under resonant interaction condition and rotating wave approximation is obtained as

$$V^{\text{int}} = -\hbar[\Omega_p e^{i(\vec{k}_p \cdot \vec{r} + \Delta_{21} t)} |2\rangle\langle 1| + \Omega_{c1} e^{i(\vec{k}_{c1} \cdot \vec{r} + \Delta_{32} t)} |3\rangle\langle 2| + \Omega_{c2} e^{i(\vec{k}_{c2} \cdot \vec{r} + \Delta_{42} t)} |4\rangle\langle 2| + \text{H.c.}], \tag{2.1}$$

where $\Delta_{21} = \omega_{21} - \omega_p$, $\Delta_{32} = \omega_{32} - \omega_{c1}$, and $\Delta_{42} = \omega_{42} - \omega_{c2}$ denote the detuning of probe and coupling field frequencies from the atomic resonance frequencies ω_{21}, ω_{32}, and ω_{42}, respectively, and $|i\rangle\langle j|$ ($i, j = 1,2,3,4$) are the atomic raising or lowering operators.

B. Density-matrix equations of motion

The time evolution of the density matrix of the system in the interaction picture is

$$\dot{\rho}_{jk} = \frac{i}{\hbar} \sum_m \left(\rho_{jm} V^{\text{int}}_{mk} - V^{\text{int}}_{jm} \rho_{mk}\right) + (\dot{\rho}_{jk})_{\text{relax}}, \quad (j,k,m = 1,2,3,4), \tag{2.2}$$

where the elements of the density matrix and interaction Hamiltonian

$$\rho_{jk} = \langle j|\rho|k\rangle \quad \text{and} \quad V^{\text{int}}_{mn} = \langle m|v^{\text{int}}|n\rangle \quad (j,k,m,n = 1,2,3,4), \tag{2.3}$$

can be calculated using the interaction Hamiltonian V^{int} given by Eq. (2.1). The second term in Eq. (2.2) includes phenomenologically, the effect of relaxation processes such as spontaneous emission $2\gamma_{jk}$ ($j, k = 1,2,3,4$) in the system. The Doppler shift of atomic resonances due to the thermal motion of the atoms in the medium gives rise to inhomogeneous broadening. To incorporate atomic motion, the derivative $\dot{\rho}_{jk}$ on the left-hand side of Eq. (2.2) can be replaced by

$$\dot{\rho}_{jk} \rightarrow \left\{\left(\frac{\partial}{\partial t}\right) + \vec{v} \cdot \vec{\nabla}\right\} \rho_{jk}, \tag{2.4}$$

where $\vec{v}$ is the atomic velocity. Time evolution of the density-matrix elements ρ_{jk} can be determined, using Eqs. (2.1), (2.3), and (2.4) in Eq. (2.2), from which using appropriate transformations to eliminate fast oscillating (exponential) terms, the equation of motion for the slowly varying components $\tilde{\rho}_{jk}$ of density-matrix elements can be obtained.

The resulting density-matrix equations for $\tilde{\rho}_{jk}$ are solved in the usual limits of a weak probe and arbitrarily strong coupling fields using the following approach. Initially all of the population is in the ground level $|1\rangle$ with a Maxwellian velocity distribution. We assume the probe to be sufficiently weak so as not to induce any population transfer to the upper levels. Thus the zeroth-order solution of the density-matrix elements

obtained in the absence of probe (i.e., setting $\Omega_p = 0$) is

$$\rho_{11}^0 = M(v), \tag{2.5}$$

where

$$M(v) = (\ln 2/\bar{v}^2\pi)^{3/2} \exp\left(\frac{-\ln 2\vec{v}\cdot\vec{v}}{\bar{v}^2}\right) \tag{2.6}$$

is the Maxwellian velocity distribution of atoms with $\bar{v} = \sqrt{\ln 2}v_{\rm th}$ and $v_{\rm th} = \sqrt{2k_BT/m_a}$ is the most probable thermal velocity at a temperature T of an atom of mass m_a. All other zeroth-order matrix elements vanish. The relevant first-order (i.e., to leading order in probe amplitude) density-matrix equations are found as

$$\dot{\tilde{\rho}}_{21}^{(1)} = -[i(\Delta_{21} + \vec{k}_p\cdot\vec{v}) + \gamma_{21}]\tilde{\rho}_{21} + i\Omega_p M(v) + i\Omega_{c1}^*\tilde{\rho}_{31}^{(1)} + i\Omega_{c2}^*\tilde{\rho}_{41}^{(1)}, \tag{2.7a}$$

$$\dot{\tilde{\rho}}_{31}^{(1)} = -\{i[(\Delta_{21} + \Delta_{32}) + (\vec{k}_p + \vec{k}_{c1})\cdot\vec{v}] + \gamma_{32}\}\tilde{\rho}_{31} + i\Omega_{c1}\tilde{\rho}_{21}^{(1)}, \tag{2.7b}$$

$$\dot{\tilde{\rho}}_{41}^{(1)} = -\{i[(\Delta_{21} + \Delta_{42}) + (\vec{k}_p + \vec{k}_{c2})\cdot\vec{v}] + \gamma_{42}\}\tilde{\rho}_{41} + i\Omega_{c2}\tilde{\rho}_{21}^{(1)}. \tag{2.7c}$$

The steady-state solution obtained by setting the time derivatives to zero on the left-hand side of Eq. (2.7) yields the velocity averaged one-photon coherence as

$$I_{21}^{(1)} = \int \tilde{\rho}_{21}^{(1)}(v)dv^3 = i\Omega_p \int dv^3\, M(v)\frac{A_{31}(v)A_{41}(v)}{A_{21}(v)A_{31}(v)A_{41}(v) + A_{31}(v)|\Omega_{c2}|^2 + A_{41}(v)|\Omega_{c1}|^2}, \tag{2.8}$$

where

$$A_{21}(v) = i(\Delta_{21} + \vec{k}_p\cdot\vec{v}) + \gamma_{21}, \tag{2.9a}$$

$$A_{31}(v) = i[(\Delta_{21} + \Delta_{32}) + (\vec{k}_p + \vec{k}_{c1})\cdot\vec{v}] + \gamma_{32}, \tag{2.9b}$$

$$A_{41}(v) = i[(\Delta_{21} + \Delta_{42}) + (\vec{k}_p + \vec{k}_{c2})\cdot\vec{v}] + \gamma_{42}. \tag{2.9c}$$

In experimental situations typically one considers an arrangement of probe and coupler fields counterpropagating along the z axis. For this experimental configuration we can henceforth set the terms $(\vec{k}_p + \vec{k}_{cj})\cdot\vec{v} = (k_p - k_{cj})v_z$, ($j$ = 1,2) and $\vec{k}_p\cdot\vec{v} = k_pv_z$ in Eqs. (2.9), and consequently the velocity integration in Eq. (2.8) reduces to a one-dimensional integral over velocity v_z.

C. Susceptibility and absorption coefficient

The susceptibility of the medium is related to the velocity averaged one-photon coherence as follows:

$$\chi = N\frac{|\mu_{21}|^2}{\hbar\gamma_D}\left(\frac{I_{21}^{(1)}}{\Omega_p/\gamma_D}\right), \tag{2.10}$$

where N is the atomic density of the vapor and $\gamma_D(=k_p\bar{v})$ is the Doppler width in the system. As is well known, the imaginary [Im(χ)] and real [Re(χ)] parts, respectively, of the susceptibility χ give the absorption and dispersion of the probe field. Transmission of the probe beam through a vapor cell of length L is governed by

$$I_p(L)/I_p(0) = \exp(\alpha_pL), \tag{2.11a}$$

where $I(L)$ and $I(0)$, respectively, are the output (at $z = L$) and input (at $z = 0$) probe beam intensities, and the probe absorption coefficient is given by

$$\alpha_p = -\frac{8\pi^2}{\lambda_p}\mathrm{Im}(\chi). \tag{2.11b}$$

D. Analytical results

For the sake of clarity and to facilitate comparison, we first analyze probe absorption (transparency) characteristics to arrive at conditions for EIT in a radiatively (homogeneously) broadened medium. The result for this case can be derived from Eq. (2.10) by dropping velocity-dependent terms and performing the velocity integration using Eq. (2.6) as follows:

$$\frac{I_{21}^{(1)}}{\Omega_p} = \frac{i}{\gamma_{21} + i\Delta_{21} + \frac{|\Omega_{c1}|^2}{\gamma_{32}+i(\Delta_{21}+\Delta_{32})} + \frac{|\Omega_{c2}|^2}{\gamma_{42}+i(\Delta_{21}+\Delta_{42})}}. \tag{2.12}$$

The above expression reveals the existence of *two* two-photon resonances in a probe absorption profile as a function of probe detuning. Evidently the one occurring at $\Delta_{21} = -\Delta_{32}$ corresponds to the transition $||1\rangle \rightarrow |2\rangle \rightarrow |3\rangle$, whereas the other occurring at $\Delta_{21} = -\Delta_{42}$ corresponds to the $|1\rangle \rightarrow |2\rangle \rightarrow |4\rangle$ transition of the four-level Y system. Thus the four-level Y system derives contributions from two distinct three-level cascade subsystems, which can be strongly coupled or decoupled by manipulating the coupling field detunings or Rabi frequencies.

For instance, let us consider the case in which both the coupling fields have the same detuning given by $\Delta(=\Delta_{32} = \Delta_{42})$. In this case a single two-photon resonance that occurs at $\Delta_{21} = -\Delta$ has contributions from both subsystems. For this case it is also clear from expression (2.12) that if the Rabi frequencies of the coupling fields are sufficiently large, so that the following criterion is met:

$$\gamma_{21} \ll \frac{|\Omega_{c1}|^2}{\gamma_{32}} + \frac{|\Omega_{c2}|^2}{\gamma_{42}}, \tag{2.13}$$

the probe absorption is considerably reduced at the position of the two-photon resonance $\Delta_{21} = -\Delta$. Furthermore, in the exact resonance case; that is, when the coupling fields are tuned to exact resonance $\Delta_{32} = \Delta_{42} = 0$, the EIT resonance is

centered around the probe detuning $\Delta_{21} = 0$. Implementation of the criterion specified in Eq. (2.13) would require choosing either very large $|\Omega_{c2}|^2$ and $|\Omega_{c1}|^2$ or very small γ_{32} and γ_{42}. Since at higher powers of the coupling fields, resolution of the Autler-Townes (AT) doublet [16], which arises from splitting of the intermediate level $|2\rangle$, tends to obfuscate the EIT effects, it is essential to choose systems in which two photon dephasing parameters γ_{32} and γ_{42} are very small in order to enable observation of EIT.

On the other hand when detuning of both the coupling fields is different, $\Delta_{32} \neq \Delta_{42}$, the two subsystems are decoupled [5,10,11] because tuning the probe frequency detuning to a particular two-photon resonance will render the other nonresonant with a large detuning. Equation (2.12) shows that then the contribution from the nonresonant term can be ignored and consequently the Y system reduces to a single three-level cascade system with absorption and dispersion properties governed by the Rabi frequency and the two-photon dephasing rate in that system.

When the medium is Doppler broadened the two-photon detuning is affected by residual Doppler broadening. The result for a Doppler broadened Y system is obtained from Eqs. (2.8) and (2.9) for counterpropagating (along the z axis) coupling and probe fields configuration as

$$\frac{I_{21}^{(1)}}{\Omega_p} = \int dv_z\, M(v_z) \frac{i}{\gamma_{21} + i(\Delta_{21} + k_p v_z) + \frac{|\Omega_{c2}|^2}{\gamma_{32} + i(\Delta_{21}+\Delta_{32}) + i(k_p - k_{c1})v_z} + \frac{|\Omega_{c1}|^2}{\gamma_{42} + i(\Delta_{21}+\Delta_{42}) + i(k_p - k_{c2})v_z}}. \tag{2.14}$$

Comparing the above result with that of a radiatively broadened case given by Eq. (2.12), we can draw the following inferences:

(i) For the case of perfect wave-vector matching, the two-photon resonances are Doppler free, $(k_p - k_{c1})v_z = (k_p - k_{c2})v_z = 0$. The criterion for observing the probe transparency at the location of two-photon resonance is still given by Eq. (2.13) but with the radiative width γ_{21} replaced by the Doppler width γ_D, i.e.,

$$\gamma_D \ll \frac{|\Omega_{c1}|^2}{\gamma_{32}} + \frac{|\Omega_{c2}|^2}{\gamma_{42}}. \tag{2.15}$$

(ii) When the detuning of both the coupling fields is different, $\Delta_{32} \neq \Delta_{42}$, the two subsystems are decoupled. The probe absorption profile then displays two distinct two-photon resonances corresponding to the individual cascade systems.

It, however, remains to be seen what happens when the probe and coupling wave vectors differ from each other. An inspection of Eq. (2.14) shows that if we consider a system in which the upper levels $|3\rangle$ and $|4\rangle$ are very close with similar decay rates, we can approximately write $\Delta_c (= \Delta_{32} \cong \Delta_{42})$, $k_c (= k_{c1} \cong k_{c2})$, and $\gamma_c (= \gamma_{32} \cong \gamma_{42})$. By using these facts in Eqs. (2.9) and through Eq. (2.8) we obtain

$$\frac{I_{21}^{(1)}}{\Omega_p} = \int dv_z\, M(v_z) \frac{i[\gamma_c + i(\Delta_{21} + \Delta_c) + i(k_p - k_c)v_z]}{[\gamma_{21} + i(\Delta_{21} + k_p v_z)][\gamma_c + i(\Delta_{21} + \Delta_c) + i(k_p - k_c)v_z)] + |\Omega_{c1}|^2 + |\Omega_{c2}|^2}. \tag{2.16}$$

Equation (2.16) resembles the typical result for a three-level cascade system [13] whose upper transition is driven by a coupling field of effective Rabi frequency $\Omega_c = \sqrt{|\Omega_{c1}|^2 + |\Omega_{c2}|^2}$. To understand the effect of velocity on probe transparency (absorption) around two-photon resonance we rewrite, by factorizing, the denominator of Eq. (2.16) in the following form:

$$\frac{I_{21}^{(1)}}{\Omega_p} = \int dv_z\, M(v_z) \frac{(\Delta_{21} + \Delta_c) + (k_p - k_c)v_z - i\gamma_c}{\left[(\Delta_{21} + \Delta_c) + (k_p - k_c)v_z - i\gamma_c - \frac{\{\Delta_c - k_c v_z + i(\gamma_{21} - \gamma_c)\}}{2}\right]^2 - \left[\sqrt{|\Omega_{c1}|^2 + |\Omega_{c2}|^2 + \frac{\{\Delta_c - k_c v_z + i(\gamma_{21} - \gamma_c)\}^2}{4}}\right]^2}. \tag{2.17}$$

Let us first analyze the above result for the matched wave vectors $k_c = k_p$ case. For this case it is easily seen that at the location of exact two-photon resonance when $\Delta_{21} = -\Delta_c$ is very close to zero, the remaining velocity and radiative width-dependent (curly brackets) terms contained in the first square bracket cancel out similar (curly brackets) terms of the second square bracket of the denominator (assuming negligible γ_c). Thus a narrow two-photon Doppler-free transparency resonance is formed around $\Delta_{21} + \Delta_c = 0$. This cancellation can no longer occur when the (nonzero) probe frequency detuning Δ_{21} is tuned away from the two-photon resonance. The residual Doppler broadening terms can then cause probe detuning Δ_{21} to shift into resonance with the absorbing AT doublet [15,17] components arising from the terms (within the second square brackets) of the denominator. Consequently in the matched wave-vector case, except in a narrow region around the two-photon resonance $\Delta_{21} + \Delta_c = 0$, at other frequencies within the region between the AT doublet, the probe is absorbed due to velocity shifting into absorbing AT doublet components.

On the other hand it is evident that if $k_p < k_c$ the residual broadening terms within the first square brackets in the

denominator tend to cancel out and thus eliminate the velocity shift of probe frequencies into absorbing AT peaks. In the extreme case of $k_c = 2\,k_p$ (which is feasible in atomic systems), the first (square brackets) term in the denominator becomes Doppler free. In other words as the probe detuning is varied the probe does not experience any (velocity-dependent) absorption for all frequencies in the entire region enclosed between the AT doublet. The frequency range over which the probe is transparent thus can be determined from the location of the AT doublet which occurs at (for the particular case when $k_c = 2\,k_p$)

$$\Delta_{21} = -\frac{\Delta_c}{2} \pm \sqrt{|\Omega_{c1}|^2 + |\Omega_{c2}|^2 + \frac{\{\Delta_c - k_c v_z\}^2}{4}}. \quad (2.18)$$

Thus we further observe that if the coupling fields are tuned to exact resonance $\Delta_c = 0$, the location of the two AT peaks is symmetric on either side of the probe resonance $\Delta_{21} = 0$. Nonzero pump detuning causes asymmetry in the AT peak positions. As is well known when the coupling fields are large compared with the Doppler width, the AT doublet will be fully resolved. This is the usual AT regime. In the typical EIT regime however, the coupling Rabi frequencies are much small compared with the Doppler width and hence the AT doublet is not resolved. Consequently the probe absorption profile should display a very broad resonance. Yet the above discussion leading to Eq. (2.18) shows that for $k_p < k_c$ it is possible to observe a wide transparency window even in the otherwise absorbing region between the AT peaks.

The foregoing explanation provides only a qualitative analysis in terms of the velocity selectivity of the EIT process associated with various wave-vector mismatch cases. We now present an analysis to obtain quantitative information regarding the nature of the width and depth of the transparency resonance and the parameter dependence of the EIT process. For this purpose the denominator of Eq. (2.16) can be factorized for velocity as

$$k_p v_z = -(\eta + \xi)/2 \pm \sqrt{[\eta - \xi]^2/4 + [|\Omega_{c1}|^2 + |\Omega_{c2}|^2]/\alpha}, \quad (2.19)$$

where

$$\xi = \Delta_{21} - i\gamma_{21}, \quad (2.20a)$$

$$\eta = (\Delta_{21} + \Delta_c - i\gamma_c)/\alpha, \quad (2.20b)$$

$$\alpha = (k_p - k_c)/k_p \neq 0. \quad (2.20c)$$

For the particular case of $k_p < k_c$ wave-vector mismatch, the sign of the residual Doppler width $(k_p - k_c)\bar{v}$ is negative. For this case we denote

$$\Phi = |k_p - k_c|/k_p = -\alpha. \quad (2.21)$$

Using Eq. (2.19) along with Eq. (2.21) in Eq. (2.16) we obtain

$$\frac{I_{21}^{(1)}}{\Omega_p} = \int \left[\frac{dv_z\, M(v_z)}{[\Delta_{21} + k_p v_z - i\gamma_{21}]}\right] \left[1 - \frac{[|\Omega_{c1}|^2 + |\Omega_{c2}|^2]/\Phi}{\left\{k_p v_z + \frac{(\eta+\xi)}{2} + i\sqrt{\frac{[|\Omega_{c1}|^2+|\Omega_{c2}|^2]}{\Phi} - \frac{[\eta-\xi]^2}{4}}\right\}\left\{k_p v_z + \frac{(\eta+\xi)}{2} - i\sqrt{\frac{[|\Omega_{c1}|^2+|\Omega_{c2}|^2]}{\Phi} - \frac{[\eta-\xi]^2}{4}}\right\}}\right]. \quad (2.22)$$

In this case it can be seen from the second term in the brackets that two poles exist: one each in the upper and lower complex (velocity) planes as long as the condition

$$\mathrm{Re}[\eta - \xi]^2/4 < [|\Omega_{c1}|^2 + |\Omega_{c2}|^2]/\Phi \quad (2.23a)$$

is fulfilled together with

$$\gamma_{21}/2, \gamma_c/2\Phi < \sqrt{[|\Omega_{c1}|^2 + |\Omega_{c2}|^2]/\Phi}. \quad (2.23b)$$

Another pole exists in the upper half plane (from the term outside the brackets). Furthermore if all the parameters are so chosen as to be much smaller compared with the Doppler width γ_D, we can approximate, $M(v) \approx \sqrt{\ln 2/\pi}\,\bar{v}^2$ in Eq. (2.22), which can then be evaluated using the method of contour integration to obtain the result

$$\frac{I_{21}^{(1)}}{\Omega_p/\gamma_D} = i\sqrt{\pi\ \ln 2}\left[1 + \frac{4\Phi[|\Omega_{c1}|^2 + |\Omega_{c2}|^2]/\{\sqrt{4\Phi[|\Omega_{c1}|^2 + |\Omega_{c2}|^2] - [(\eta - \xi)\Phi]^2}\}}{\{i(\eta - \xi)\Phi - \sqrt{4\Phi[|\Omega_{c1}|^2 + |\Omega_{c2}|^2] - [(\eta - \xi)\Phi]^2}\}}\right]. \quad (2.24)$$

Furthermore, using the condition (2.23b) to ignore γ_c, $\Phi\gamma_{21}$ in η and ξ [defined in Eqs. (2.20)] the above result, Eq. (2.24), is recast in terms of real and imaginary parts as

$$\frac{I_{21}^{(1)}}{\Omega_p/\gamma_D} = i\sqrt{\pi\ \ln 2}\left[1 + \frac{i(\Delta_{21} + \Delta_c + \Delta_{21}\Phi) - \sqrt{4\Phi[|\Omega_{c1}|^2 + |\Omega_{c2}|^2] - [\Delta_{21} + \Delta_c + \Delta_{21}\Phi]^2}}{\sqrt{4\Phi[|\Omega_{c1}|^2 + |\Omega_{c2}|^2] - [\Delta_{21} + \Delta_c + \Delta_{21}\Phi]^2}}\right]. \quad (2.25)$$

The above result shows that the probe absorption described by the imaginary part of Eq. (2.25) is zero as long as the condition $(\Delta_{21} + \Delta_c + \Delta_{21}\Phi) < \sqrt{4\Phi[|\Omega_{c1}|^2 + |\Omega_{c2}|^2]}$ [stipulated by Eq. (2.23a)] is fulfilled. Clearly the full width of this transparency region is given by

$$\gamma_t = 2\sqrt{4\Phi[|\Omega_{c1}|^2 + |\Omega_{c2}|^2]}. \quad (2.26)$$

It is interesting to note that the width of the transparency region depends upon the wave-vector mismatch and increases as $\sqrt{\Phi}$ for given coupling field powers. Thus if $\Phi = 1$, which corresponds to the wave-vector mismatch situation of $k_c = 2\ k_p$, almost an entire region between the AT doublet can be rendered transparent [see also the discussion preceding Eq. (2.18)]. Eqs. (2.26) and (2.24) are the main new results of the present work which allow us to estimate the depth and width of the transparency windows for a cascade-type three-level system in which $k_c > k_p$.

III. NUMERICAL RESULTS AND DISCUSSIONS

We now present the numerical results for EIT by applying the theory to a typical experimental situation in which probe and coupler fields counterpropagating along the z axis are incident on a cell containing atomic vapor. For this configuration the numerical results are obtained by performing one-dimensional velocity integration of Eq. (2.8) using Eqs. (2.9) and (2.6), and subsequently using Eqs. (2.10) and (2.11) to obtain, respectively, the susceptibility and transmission of the probe. As mentioned earlier for counterpropagating probe and coupling waves, the nature of EIT in a three-level cascade system depends critically on the relative sign of the residual Doppler width $(k_p - k_c)\bar{v}$ which, depending on the probe and coupling field wave-vector mismatch, can be positive $(k_p > k_c)$ or negative $(k_p < k_c)$ and is markedly dissimilar from each other. If the wave vectors k_p and k_c are the same in magnitude $(k_p = k_c)$, the residual Doppler width vanishes, and usually the medium is considered to be Doppler free.

Keeping in mind the essential criterion (2.15) for the observation of EIT as well as the wave-vector mismatch condition (2.21), for our numerical calculations we have chosen an atomic system in which $k_p < k_{ci}$ (or $\lambda_p > \lambda_{ci}$) (where $ci = c1, c2$), so the sign of the residual Doppler width is negative. This situation can be realized, for example, considering the transitions $3\ S_{1/2} \rightarrow 3\ P_{3/2} \rightarrow 4\ D_{3/2}$ ($3\ S_{1/2} \rightarrow 3\ P_{3/2} \rightarrow 4\ D_{5/2}$) in a sodium atom. These transitions form a four-level dual cascade (Y-type) EIT configuration with one stable ground state $3\ S_{1/2}$, an intermediate level $3\ P_{3/2}$, and two nearly degenerate upper states $4\ D_{3/2}$ and $4\ D_{5/2}$. The level separation wavelength of the lower and intermediate levels is $\lambda_p = 5890$ Å (D_2 transition) and those of the intermediate and upper transitions are $\lambda_{c1} \cong \lambda_{c2} = 5688$ Å. The large wavelength mismatch between the counterpropagating coupling and probe fields in this dual ladder EIT system introduces a residual Doppler width $(k_p - k_c)\bar{v}/k_p\bar{v} \simeq -0.04$. For comparison purposes the other case of matched $(k_p = k_c)$ [and positive $(k_p > k_c)$] wave-vector mismatch is also considered hypothetically for this four-level Y-type atomic system. In our numerical calculation all parameters are expressed in units of Doppler width $\gamma_D/2\pi = 1$ GHz, i.e., $2\gamma_{21}/\gamma_D = 0.01$, $2\gamma_{32}/\gamma_D = 0.0003$, and $2\gamma_{42}/\gamma_D = 0.0019$.

In Fig. 2(i) probe absorption [Im $(I_{21}^{(1)}\gamma_D/\Omega_p)$] and dispersion [Re $(I_{21}^{(1)}\gamma_D/\Omega_p)$] profiles are shown as a function of the probe detuning for various cases of coupling and probe field wave-vector mismatches. The coupling fields are on resonance $(\Delta_{32} = \Delta_{32} = 0)$ and the Rabi frequencies are chosen equal

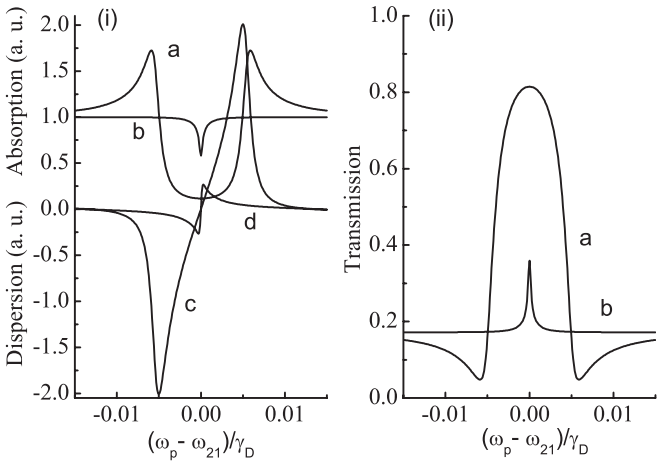

FIG. 2. (i) Probe absorption (curves a, b) and dispersion (curves c, d) in arbitrary units (a.u.) as a function of probe field detuning $(\omega_p - \omega_{21})/\gamma_D$ with coupling field Rabi frequencies $\Omega_{c1} = \Omega_{c2} = 10\ (2\pi \times \text{MHz})$ and for various wave-vector mismatch cases for $k_p - k_c = -0.04\ k_p$ (curves a and c) and $k_p = k_c$ (curves b and d). The coupling fields are on resonance $(\Delta_{32} = \Delta_{42} = 0)$. (ii) Probe transmission $[I_p(L)/I_p(0)]$ as a function of the probe detuning for wave-vector mismatch $k_p - k_c = -0.04\ k_p$ (curve a) and $k_p = k_c$ (curve b). Thus the values of unity and zero on the y axis (in this and subsequent figures) correspond, respectively, to the maximum $[I_p(L) = I_p(0)]$ and minimum $[I_p(L) = 0]$ transmission of probe intensity. The density-length product [used in Eqs. (2.11)] is NL $= 2 \times 10^{11}$ atoms/cm^2 and other parameters are the same as in (i).

$(\Omega_{c1} = \Omega_{c2})$ and of the same magnitude as the spontaneous emission rate of the probe transition $2\gamma_{21}(=2\pi \times 10$ MHz). No transparency is found to exist for the $k_p > k_c$ wave-vector mismatch case (hence results are not shown). There is no perfect EIT even in the exact wave-vector matching $(k_p = k_c)$

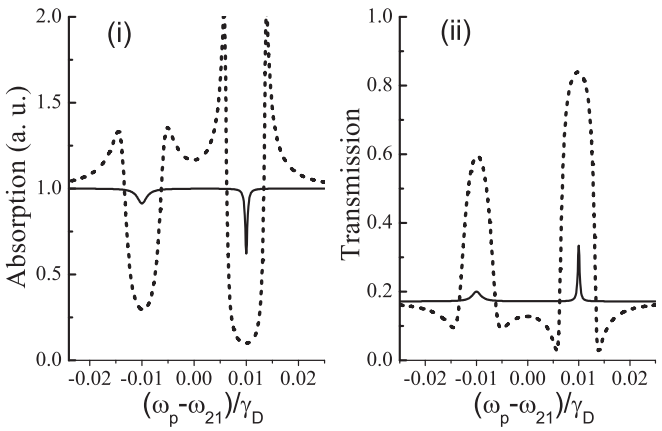

FIG. 3. (i) Probe absorption (a.u.) as a function of the probe field detuning $(\omega_p - \omega_{21})/\gamma_D$ for the coupling field Rabi frequencies $\Omega_{c1} = \Omega_{c2} = 10\ (2\pi \times \text{MHz})$ and various wave-vector mismatch cases, $k_p - k_c = -0.04\ k_p$ (dashed line) and $k_p = k_c$ (solid line). The coupling fields detuning chosen are $\Delta_{42} = -\Delta_{32} = 10\ (2\pi \times \text{MHz})$. (b) Probe transmission $[I_p(L)/I_p(0)]$ as a function of the probe detuning for density-length product, NL $= 2 \times 10^{11}$ atoms/cm^2, and the same parameters as in (i).

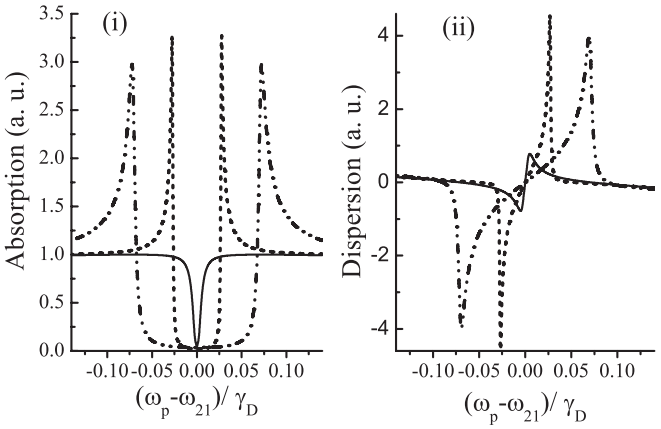

FIG. 4. Probe (i) absorption and (ii) dispersion (a.u.) as a function of the probe field detuning $(\omega_p - \omega_{21})/\gamma_D$ for strong coupling field Rabi frequencies $\Omega_{c1} = \Omega_{c2} = 50$ $(2\pi \times \text{MHz})$ and various wave-vector mismatch cases, $k_p - k_c = -0.04\, k_p$ (dashed line) and $k_p = k_c$ (solid line). Also shown is the case when $k_c = 2\, k_p$ (dashed-dot-dot line).

case (curves b and d). It should be noted that for these values $(2\pi \times 10$ MHz) of the coupling field Rabi frequencies the criterion for observing the EIT specified by Eq. (2.15) is not fulfilled. Yet a very wide and almost complete transparency window appears in the case when $k_p < k_c$ (curves a and c). The width of this resonance is in good agreement with the analytical result given by Eq. (2.26). The EIT resonance and the dispersion curves for the $k_p = k_c$ case are narrower than those observed for $k_p < k_c$ since in the former case it is governed mainly by the two-photon dephasing rate alone for small values of coupling Rabi frequencies, whereas in the latter case it depends [see Eq. (2.26)] on the mismatch factor $k_p - k_c$ and the Rabi frequency of the coupling fields. Figure 2(ii) shows the probe transmission [using Eqs. (2.11)] as a function of the probe detuning for the same parameters as in Fig. 2(i). The density-length product used is NL $= 2 \times 10^{11}$ atoms/cm ^{2}. The transmission at line center for $k_p < k_c$ (curve a) is very high as compared with the matched $k_p = k_c$ case (curve b).

We now consider the finite detuning case when the coupling fields are detuned on either side of the intermediate level. Figure 3(i) shows the probe absorption [Im $(I_{21}^{(1)}\gamma_D/\Omega_p)$] and dispersion [Re $(I_{21}^{(1)}\gamma_D/\Omega_p)$] variation as the probe frequency is tuned through the coupling field detuning. The probe absorption profile for this case splits into two distinct transparency windows corresponding to two distinct cascade subsystems. The transparency window occurring at the two-photon resonance $\Delta_{21} + \Delta_{32} = 0$ corresponds to the 3 $S_{1/2} \rightarrow$ 3 $P_{3/2} \rightarrow 4$ $D_{3/2}$ transition, whereas the other occurring at $\Delta_{21} + \Delta_{42} = 0$ corresponds to the 3 $S_{1/2} \rightarrow 3$ $P_{3/2} \rightarrow 4$ $D_{5/2}$ transition. Since these two cascade subsystems are decoupled, the depth and width of each transparency window is now governed by the two-photon dephasing rate parameter and the coupling field Rabi frequency in that particular subsystem. The asymmetry in the depth of the transparency in the two windows occurs as the two-photon decay rates in the two subsystems are dissimilar in the present Y system. The probe transmission shown in Fig. 3(ii) also displays similar features.

Finally in Fig. 4 we show the probe absorption and dispersion profile choosing values of the coupling field Rabi frequencies $\Omega_{c1} = \Omega_{c2} = 50$ $(2\pi \times$ MHz) which fulfill the criterion (2.15) for observing large absorption reduction at line center. The coupling fields are on resonance $(\Delta_{32} = \Delta_{32} = 0)$. As usual in the matched wave-vector $(k_c = k_p)$ case we observe a narrow resonance and complete transparency at the probe line center. For illustration purposes also shown is the result when $k_c = 2k_p$ (hypothetical case). In this case it is evident that the width of the transparency window [as predicted by Eq. (2.25)] is the same as the separation between the AT peaks and hence the entire region between the AT doublet is rendered transparent.

IV. CONCLUSION

We have studied the EIT of a probe field in both homogeneously (radiative) and Doppler broadened four-level Y-type atomic systems driven by two strong laser (coupling) fields. The influence of residual Doppler broadening on two-photon resonances was assessed for various wave-vector mismatches occurring when the frequency of coupling fields is higher $(k_c > k_p)$, equal $(k_c = k_p)$, or lesser $(k_c < k_p)$ than that of the probe field frequency. Contrary to the usual belief, it is found that in the $k_c > k_p$ wave-vector mismatch case the residual Doppler broadening is actually conducive for the observation of transparency in Doppler broadened four-level Y-type atomic systems. In this case, the probe absorption profile displays very wide and almost completely transparent single or double EIT windows whose width, depth, and location depend on the wave-vector mismatch, Rabi frequencies, and atom field detuning of the coupling fields. Thus it is possible to attain almost complete transparency over a broad range of frequencies which may be essential for propagation of very short light pulses through an inhomogeneously broadened medium. Analytical results derived to explain the velocity selective nature of transparency (absorption) and the width of resonances are in good agreement with computed results.

[1] J. E. Field, K. H. Hahn, and S. E. Harris, Phys. Rev. Lett. **67**, 3062 (1991); S. E. Harris, Phys. Today **50**, 36 (1997).

[2] L. V. Hau, S. E. Harris, Z. Dutton, and C. H. Behroozi, Nature (London) **397**, 594 (1999); A. M. Akulshin, S. Barreiro, and A. Lezama, Phys. Rev. A **57**, 2996 (1998).

[3] M. Fleischhauer and M. D. Lukin, Phys. Rev. Lett. **84**, 5094 (2000).

[4] P. R. Hemmer, D. P. Katz, J. Donoghue, M. Cronin-Golomb, M. S. Shahriar, and P. Kumar, Opt. Lett. **20**, 982 (1995).

[5] G. S. Agarwal and W. Harshawardhan, Phys. Rev. Lett. **77**, 1039 (1996).

[6] J. Y. Gao, S. H. Yang, D. Wang, X. Z. Guo, K. X. Chen, Y. Jiang, and B. Zhao, Phys. Rev. A **61**, 023401 (2000).

[7] D. Wang, J. Y. Gao, J. H. Xu, G. La Rocca, and F. Bassani, Europhys. Lett. **54**, 456 (2001); J. H. Xu, G. C. La Rocca,

F. Bassani, D. Wang, and J. Y. Gao, Opt. Commun. **216**, 157 (2003).

[8] R. Arun, Phys. Rev. A **77**, 033820 (2008).

[9] B. P. Hou, S. J. Wang, W. L. Yu, and W. L. Sun, Phys. Rev. A **69**, 053805 (2004); B. K. Dutta and P. K. Mahapatra, J. Phys. B: At., Mol. Opt. Phys. **41**, 055501(2008).

[10] Y. Zhang, A. W. Brown, and M. Xiao, Phys. Rev. Lett. **99**, 123603 (2007).

[11] Y. Zhang, B. Anderson, A. W. Brown, and M. Xiao, Appl. Phys. Lett. **91**, 061113 (2007).

[12] L. G. Si, X. Y. Lu, X. Hao, and J. H. Li, J. Phys. B: At., Mol. Opt. Phys. **43**, 065403 (2010).

[13] J. Gea-Banacloche, Y. Q. Li, S. Z. Jin, and M. Xiao, Phys. Rev. A **51**, 576 (1995).

[14] D. J. Fulton, S. Shepherd, R. R. Moseley, B. D. Sinclair, and M. H. Dunn, Phys. Rev. A **52**, 2302 (1995).

[15] S. Shepherd, D. J. Fulton, and M. H. Dunn, Phys. Rev. A **54**, 5394 (1996); J. R. Boon, E. Zekou, D. McGloin, and M. H. Dunn, *ibid*. **59**, 4675 (1999).

[16] F. Silva, J. Mompart, V. Ahufinger, and R. Corbalan, Eurphys. Lett. **51**, 286 (2000); Phys. Rev. A **64**, 033802 (2001).

[17] S. H. Autler and C. H. Townes, Phys. Rev. **100**, 703 (1955).